Inorganica Chimica Acta 386 (2012) 83–92

Contents lists available at SciVerse ScienceDirect

Inorganica Chimica Acta

journal homepage: www.elsevier.com/locate/ica

Synthesis of zinc and cadmium *O*-alkyl thiocarbonate and dithiocarbonate complexes and a cationic zinc hydrosulfide complex

Nicholas G. Spiropulos [a], Eric A. Standley [a], Ian R. Shaw [a], Benjamin L. Ingalls [a], Bryan Diebels [a], Sylvanna V. Krawczyk [b], Benjamin F. Gherman [b], Atta M. Arif [c], Eric C. Brown [a,*]

[a] Department of Chemistry and Biochemistry, 1910 University Drive, Boise State University, Boise, ID 83725, USA
[b] Department of Chemistry, 6000 J Street, California State University, Sacramento, Sacramento, CA 95819, USA
[c] Department of Chemistry, University of Utah, Salt Lake City, UT 84112, USA

ARTICLE INFO

Article history:
Received 8 August 2011
Received in revised form 16 January 2012
Accepted 20 January 2012
Available online 9 February 2012

Keywords:
Heterocumulenes
Zinc
Cadmium
Hydrosulfide
Crystal structures
DFT calculations

ABSTRACT

Treatment of Zn(II) and Cd(II) hydroxide complexes of the tris(2-pyridylmethyl)amine (TPA) ligand with COS or CS_2 in protic solvents (MeOH or EtOH) resulted in [(TPA)Zn–SC(S)OCH_3]ClO_4 (**1**), [(TPA)Zn–SC(O)OCH_3]BF_4 (**2**), [(TPA)Zn–SC(O)OCH_3]ClO_4 (**3**), [(TPA)Zn–SC(O)OCH_2CH_3]BF_4 (**4**), [(TPA)Cd–SC(S)OCH_3]ClO_4 (**5**) and [(TPA)Cd–SC(O)OCH_3]ClO_4 (**6**). The molecular structures of **1**, **2**, **5** and **6** were determined by X-ray crystallography. Complexes **2**, **3** and **4**, unlike **1**, **5** and **6**, are easily hydrolyzed upon treatment with water in CH_3CN to give zinc hydrosulfide complexes of the form [(TPA)Zn–SH]X (X = BF_4^- (**7**) and ClO_4^- (**8**)), as evidenced by spectroscopic methods and the crystal structure of **7**. These complexes may be prepared more directly by (a) reacting equimolar amounts of TPA, $Zn(ClO_4)_2{\cdot}6H_2O$ and $Me_4NOH{\cdot}5H_2O$ with COS in CH_3CN or (b) treating [$((TPA)Zn)_2(\mu\text{-}OH)_2$]$(ClO_4)_2$ with H_2S. Moreover, reactivity and density functional theory computational studies comparing the cationic hydrosulfide complexes **7** and **8** with the neutral zinc hydrosulfide complexes supported by tris(pyrazolyl)borate ligands have been conducted and subtle differences between the two types of hydrosulfide complexes have been determined.

1. Introduction

Extensive research efforts have been directed at understanding carbon dioxide (CO_2) insertion into coordination complexes because of its biological significance to carbonic anhydrase (CA) [1]. CA, which is a zinc-containing enzyme common to animals, plants and bacteria, catalyzes the reversible hydration of CO_2 to bicarbonate [2]. The enzyme is involved in numerous processes within living organisms, such as cellular respiration, photosynthesis, and pH regulation [3]. However, research aimed at understanding insertion of sulfur-containing heterocumulenes, such as carbonyl sulfide (COS) and carbon disulfide (CS_2), into zinc-containing complexes has been rather limited [4,5]. This is surprising since studies have shown atmospheric COS is fixated by CA in plants, lichens and algae [6] and CS_2 is fixated by CS_2 hydrolase (3TEN), a zinc-containing enzyme similar to CA, in thermophilic archaea [7]. Furthermore, few studies [8] have examined heterocumulene insertion into cadmium-containing complexes, even though a cadmium carbonic anhydrase (3BOB) is formed by marine diatoms in zinc-poor environments [9].

The active site of CA consists of a tetrahedral Zn^{2+} ion coordinated by three histidine residues (His-94, His-96 and His-119) and a water molecule [10]. The proposed mechanism of COS fixation by CA [4], which is shown in Scheme 1, involves deprotonation of the coordinated water molecule ($pK_a \approx 7$) to form a zinc hydroxide complex (**B**). Insertion of COS into the metal–hydroxide bond results in the formation of $[(His)_3Zn\text{–}SC(O)OH]^+$ (**C**) that readily decomposes to form the cationic zinc hydrosulfide complex $[(His)_3Zn\text{–}SH]^+$ (**D**). The proposed final step is protonation of the hydrosulfide ligand and release of H_2S at neutral pH. However, many questions remain unresolved regarding desulfurization of the zinc hydrosulfide complex (**D**) and how it occurs near a neutral pH.

Prior studies by Parkin and co-workers [11], Vahrenkamp and co-workers [5,12] and Anders and co-workers [13] to make $[(L)Zn\text{–}SH]^n$ (where $n = 0$ or +1) complexes, akin to intermediate **D** in Scheme 1, made use of substituted tris(pyrazolyl)borate ($Tp^{R,Me}$) and neutral azamacrocyclic ([12]aneN$_3$) tripodal ligands (Chart 1). The authors found that the $Tp^{R,Me}$ ligand was the only ligand capable of stabilizing the $[Zn\text{–}SH]^+$ moiety [14]. For instance, an attempt by Ender et al. to make a cationic $[([12]aneN_3)Zn\text{–}SH]^+$ complex with the neutral [12]aneN$_3$ ligand (Chart 1) resulted in ZnS formation [13]. As such, a number of $Tp^{R,Me}$Zn–SH complexes supported with different substituted pyrazolylborate ligands have been characterized [5,11,12]. The remarkable stability of the $Tp^{R,Me}$Zn–SH complexes

* Corresponding author. Tel.: +1 208 426 1186; fax: +1 208 426 3027.
E-mail address: ericbrown3@boisestate.edu (E.C. Brown).

0020-1693/$ - see front matter © 2012 Elsevier B.V. All rights reserved.
http://dx.doi.org/10.1016/j.ica.2012.01.040

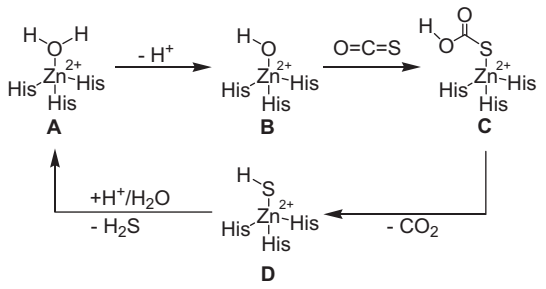

Scheme 1. Proposed catalytic mechanism of COS hydrolysis by carbonic anhydrase.

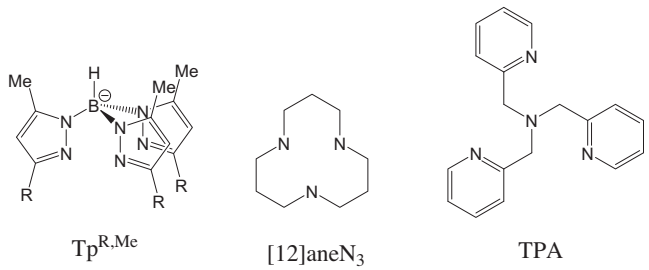

Chart 1. Ligands used or cited in this work.

has been attributed to the ability of the $Tp^{R,Me}$ ligand to encapsulate the labile hydrosulfide ligand and, thus, prevent demetallation and formation of insoluble zinc sulfides.

The tris(2-pyridylmethyl)amine (TPA) ligand (Chart 1) was chosen as the supporting ligand in this study primarily because $[((TPA)Zn)_2(\mu\text{-}OH)_2](ClO_4)_2$ has already been shown to undergo insertion reactions with heterocumulenes, such as CO_2, under basic conditions [15]. Additional reasons why we chose to use the TPA ligand is that (a) it can be modified with steric substituents [16] and hydrogen bond donors [17] and (b) it would result in a cationic rather than a neutral hydrosulfide complex. TPA has the advantage of yielding a cationic active site model, rather than Tp which is an anionic biomimetic ligand. As such, there is potential with TPA to better model the CA chemistry.

Herein, we describe the insertion reactions of $[((TPA)M)_2(\mu\text{-}OH)_2]^{2+}$ where M = Zn, Cd with CS_2 and COS in protic (MeOH, EtOH) and aprotic solvents (CH_3CN). Overall, *O*-alkyl dithiocarbonate and thiocarbonate complexes are formed under protic conditions (MeOH and EtOH). Particularly important, complexes $[(TPA)Zn\text{–}SC(O)OMe]^+$ and $[(TPA)Cd\text{–}SC(O)OMe]^+$ were formed and, according to the Cambridge Structural Database, represent the first structurally characterized examples of Zn or Cd complexes containing an M–SC(O)OR fragment. In addition, new synthetic methods under aprotic (CH_3CN) conditions resulted in cationic complexes of the general formula $[(TPA)Zn\text{–}SH]^+$. These complexes were characterized by ^1H and ^{13}C NMR, IR, and electrospray mass spectrometry (ESI-MS) and, in one example, by X-ray crystallography. Furthermore, theoretical calculations were used to compare the electronics and predict the reactivity of the TPA/Tp ZnSH complexes. Taken together, the results provide new detail for routes to synthetic Zn–SH complexes and the relative characteristics of the two predominant CA models (Tp and TPA).

2. Experimental

2.1. General data

All reactions were performed using standard Schlenk techniques under an atmosphere of dry nitrogen gas. Solvents and reagents were obtained from commercial sources in analytical grade quality and used as received unless noted otherwise. The solvents tetrahydrofuran (THF), methanol (MeOH), ethanol (EtOH) and acetonitrile (CH_3CN) were dried with CaH_2 and distilled prior to use. NMR spectra were recorded on a Bruker AVANCE III 600 NMR. Chemical shifts (δ) for ^1H or ^{13}C NMR spectra were referenced to residual protium in the deuterated solvent. IR spectra were measured using a Perkin Elmer Spectrum 100 spectrometer. Elemental analyses were performed by Atlantic Microlabs of Norcross, GA. High resolution electrospray mass spectra were recorded on a Bruker Daltonics Maxis QTOF instrument. The ligand tris(2-pyridylmethyl)amine (TPA) was made by following a previously reported procedure [18].

2.2. Synthesis and characterization

2.2.1. Preparation of $[(TPA)ZnSC(S)OMe]ClO_4$, (**1**)

To a solution of tris(2-pyridylmethyl)amine (290 mg, 1.00 mmol) dissolved in dry methanol (40 mL) was added $Zn(ClO_4)_2{\cdot}6H_2O$ (373 mg, 1.00 mmol). After stirring for 5 min, KOH (56 mg, 1.00 mmol) was added which caused immediate formation of a white precipitate. Carbon disulfide (228 mg, 3.00 mmol) was then added and the reaction was stirred overnight. The solvent was removed under reduced pressure and the residue extracted with dichloromethane (15 mL) and filtered through Celite. The volume was reduced (~3 mL) and addition of diethyl ether (20 mL) caused the formation of a pale yellow solid. The solid was collected, washed with diethyl ether (10 mL) and dried under vacuum (409 mg, 75%). Colorless crystals suitable for crystallographic characterization were obtained by diethyl ether diffusion into acetonitrile at room temperature. ^1H NMR (CD_3CN, 600 MHz): δ 8.72 (d, 3H), 8.06 (t, 3H), 7.59 (t, 3H), 7.54 (d, 3H), 4.24 (s, 6H), 3.87 (s, 3H). ^{13}C NMR (CD_3CN, 150 MHz): δ 225.2, 155.0, 148.6, 141.2, 125.0, 124.6, 60.07, 56.97. IR (ATR, cm^{-1}): 2981, 1609, 1576, 1485, 1446, 1436, 1373, 1314, 1295, 1272, 1199, 1131, 1111, 1081, 1066, 1052, 1022, 1001, 990, 944, 907, 836, 774, 761, 732, 719. *Anal.* Calc. for $C_{20}H_{21}ZnClN_4O_5S_2$: C, 42.71; H, 3.76; N, 9.96. Found: C, 42.52; H, 3.71; N, 9.84%.

2.2.2. Preparation of $[(TPA)ZnSC(O)OMe]BF_4$, (**2**)

To a solution of tris(2-pyridylmethyl)amine (800 mg, 2.80 mmol) dissolved in dry methanol (50 mL) was added zinc tetrafluoroborate (658 mg, 2.80 mmol). After stirring for 5 min, KOH (155 mg, 2.80 mmol) was added and the headspace gases were removed by vacuum. Carbonyl sulfide was then bubbled through the solution and the reaction was allowed to stir under a COS atmosphere for 24 h at room temperature, during which time a white precipitate formed. The solid was collected and extracted with dichloromethane (2 × 20 mL). The dichloromethane solution was concentrated (5 mL) and addition of diethyl ether (20 mL) resulted in a pale yellow solid. The solid was collected, washed with diethyl ether (3 mL) and dried under vacuum (602 mg, 41%). Colorless crystals suitable for crystallographic characterization were obtained by diethyl ether diffusion into methanol at room temperature. ^1H NMR (CD_3CN, 600 MHz): δ 8.73 (d, 3H), 8.07 (t, 3H), 7.61 (t, 3H), 7.57 (d, 3H), 4.19 (s, 6H), 3.57 (s, 3H). ^{13}C NMR (CD_3CN, 150 MHz): δ 176.5, 155.2, 148.9, 141.2, 125.0, 124.7, 56.3, 52.8. IR (ATR, cm^{-1}): 2946, 1647, 1609, 1575, 1482, 1435, 1375, 1319, 1298, 1273, 1184, 1164, 1114, 1048, 1022, 978, 956, 909, 835, 812, 770, 73, 687. *Anal.* Calc. for $C_{20}H_{21}ZnBF_4N_4O_2S$: C, 45.01; H, 3.97; N, 10.50. Found: C, 44.84; H, 4.01; N, 10.53%.

2.2.3. Preparation of $[(TPA)ZnSC(O)OMe]ClO_4$, (**3**)

To a solution of tris(2-pyridylmethyl)amine (250 mg, 0.86 mmol) dissolved in dry methanol (40 mL) was added $Zn(ClO_4)_2{\cdot}6H_2O$ (320 mg, 0.86 mmol). After stirring for 5 min, KOH (48 mg, 0.86 mmol) was added and the headspace gases were

removed by vacuum. Carbonyl sulfide was then bubbled through the solution and the reaction was allowed to stir under a COS atmosphere for 24 h at room temperature, during which time a white precipitate formed. The solid was collected and extracted with dichloromethane (20 mL). The dichloromethane solution was concentrated (~5 mL) and addition of diethyl ether (15 mL) resulted in a pale yellow solid. The solid was collected, washed with diethyl ether (5 mL) and dried under vacuum (138 mg, 30%). ^{1}H NMR (CD_3CN, 600 MHz): δ 8.63 (d, 3H), 8.02 (t, 3H), 7.57 (t, 3H), 7.53 (d, 3H), 4.10 (s, 6H), 3.67 (s, 3H). ^{13}C NMR (CD_3CN, 150 MHz): δ 178.4, 154.8, 149.4, 140.5, 125.2, 125.0, 57.0, 53.7. IR (ATR, cm^{-1}): 2943, 2013, 1646, 1609, 1575, 1487, 1453, 1435, 1375, 1318, 1298, 1272, 1185, 1161, 1129, 1114, 1081, 1052, 1024, 976, 956, 909, 838, 814, 768, 730, 686. *Anal.* Calc. for $C_{20}H_{21}ZnClN_4O_6S$: C, 43.97; H, 3.87; N, 10.26. Found: C, 43.69; H, 3.94; N, 10.10%.

2.2.4. Preparation of [(TPA)ZnSC(O)OEt]BF_4, (**4**)

To a solution of tris(2-pyridylmethyl)amine (250 mg, 0.86 mmol) dissolved in dry ethanol (50 mL) was added zinc tetrafluoroborate (206 mg, 0.86 mmol). After the addition of KOH (48 mg, 0.86 mmol), the headspace gases were removed by vacuum. Carbonyl sulfide was then bubbled through the solution and the reaction was allowed to stir under a COS atmosphere for 24 h at room temperature. The solvent was then removed under reduced pressure and the residue extracted with dichloromethane (10 mL) and filtered through Celite. The dichloromethane solution was concentrated (3 mL) and addition of diethyl ether (20 mL) resulted in a white solid. The solid was collected, washed with diethyl ether (3 mL) and dried under vacuum (150 mg, 32%). ^{1}H NMR (CD_3CN, 600 MHz): δ 8.73 (d, 3H), 8.07 (t, 3H), 7.61 (t, 3H), 7.55 (d, 3H), 4.19 (s, 6H), 3.98 (q, 2H), 0.92 (t, 3H). ^{13}C NMR (CD_3CN, 150 MHz): δ 175.7, 155.2, 148.9, 141.2, 125.0, 124.7, 61.9, 56.3, 13.4. IR (ATR, cm^{-1}): 3435, 2963, 2870, 1543, 1461, 1362, 1316, 1294, 1253, 1230, 1202, 1128, 1082, 1047, 1023, 997, 950, 876, 851, 810, 748, 734, 723, 690. All attempts to obtain analytically pure material were not possible for this compound. As evidenced by ^{1}H NMR, samples always included small amounts of [(TPA)Zn–SH]ClO_4 (**8**) resulting from the hydrolysis of **4**.

2.2.5. Preparation of [(TPA)CdSC(S)OMe]ClO_4, (**5**)

To a solution of tris(2-pyridylmethyl)amine (250 mg, 0.86 mmol) dissolved in dry methanol (40 mL) was added $Cd(ClO_4)_2{\cdot}6H_2O$ (360 mg, 0.86 mmol). After stirring for 5 min, KOH (48 mg, 0.86 mmol) was added which caused immediate formation of a white precipitate. Carbon disulfide (328 mg, 5.00 mmol) was then added and the reaction was stirred overnight. The solvent was removed under reduced pressure and the residue extracted with dichloromethane (15 mL) and filtered through Celite. The volume was reduced (~3 mL) and addition of diethyl ether (15 mL) caused the formation of a pale yellow solid. The solid was collected, washed with diethyl ether (5 mL) and dried under vacuum (213 mg, 41%). Colorless crystals suitable for crystallographic characterization were obtained by pentane diffusion into dichloromethane at room temperature. ^{1}H NMR (CD_3CN, 600 MHz): δ 8.76 (d, 3H), 8.00 (t, 3H), 7.56 (t, 3H), 7.51 (d, 3H), 4.17 (s, 6H), 4.12 (s, 3H). ^{13}C NMR (CD_3CN, 150 MHz): δ 230.7, 154.8, 149.4, 140.3, 125.0, 124.9, 63.5, 57.3. IR (ATR, cm^{-1}): 2942, 1642, 1605, 1576, 1483, 1435, 1373, 1313, 1271, 1204, 1147, 1074, 1051, 1018, 899, 835, 767, 733. *Anal.* Calc. for $C_{20}H_{21}CdClN_4O_5S_2$: C, 39.42; H, 3.47; N, 9.19. Found: C, 39.19; H, 3.48; N, 9.00%.

2.2.6. Preparation of [(TPA)CdSC(O)OMe]ClO_4, (**6**)

To a solution of tris(2-pyridylmethyl)amine (300 mg, 1.03 mmol) dissolved in dry methanol (40 mL) was added $Cd(ClO_4)_2{\cdot}6H_2O$ (433 mg, 1.03 mmol). After the addition of KOH (58 mg, 1.03 mmol), the headspace gases were removed by vacuum. Carbonyl sulfide was then bubbled through the solution and the reaction was allowed to stir under a COS atmosphere for 8 h at room temperature, during which time a white precipitate formed. The solution was filtered and the filtrate solvent was removed under reduced pressure. The residue was extracted with dichloromethane (20 mL) and filtered through Celite. The dichloromethane solution was concentrated (3 mL) and addition of diethyl ether (20 mL) resulted in a white solid. The solid was collected, washed with diethyl ether (3 mL) and dried under vacuum (162 mg, 27%). Colorless crystals suitable for crystallographic characterization were obtained by diethyl ether diffusion into methanol at room temperature. ^{1}H NMR (CD_3CN, 600 MHz): δ 8.64 (d, 3H), 8.03 (t, 3H), 7.57 (t, 3H), 7.52 (d, 3H), 4.10 (s, 6H), 3.67 (s, 3H). ^{13}C NMR (CD_3CN, 150 MHz): δ 178.4, 154.8, 149.5, 140.5, 125.2, 125.0, 57.0, 53.7. IR (ATR, cm^{-1}): 3564, 3093, 2950, 2013, 1636, 1604, 1575, 1484, 1442, 1428, 1372, 1317, 1301, 1267, 1191, 1125, 1077, 1053, 1017, 1002, 982, 963, 903, 891, 836, 816, 768, 737, 687. *Anal.* Calc. for $C_{20}H_{21}CdClN_4O_6S{\cdot}CH_3OH$: C, 40.33; H, 4.03; N, 8.96. Found: C, 39.82; H, 3.61; N, 9.39%.

2.2.7. Preparation of [(TPA)ZnSH]BF_4, (**7**)

To a solution of tris(2-pyridylmethyl)amine (250 mg, 0.86 mmol) dissolved in dry methanol (30 mL) was added zinc tetrafluoroborate (206 mg, 0.86 mmol). After the addition of KOH (48 mg, 0.86 mmol), the headspace gases were removed by vacuum. Hydrogen sulfide was then bubbled through the solution and the reaction was allowed to stir under a H_2S atmosphere for 24 h at room temperature, during which time a white precipitate formed. The solid was collected and extracted with dichloromethane (2 × 10 mL). The dichloromethane solution was concentrated (5 mL) and addition of diethyl ether (20 mL) resulted in a white solid. The white solid was collected, washed with diethyl ether (5 mL) and dried under vacuum (160 mg, 39%). Colorless crystals suitable for crystallographic characterization were obtained by diethyl ether diffusion into THF at room temperature. ^{1}H NMR (CD_3CN, 600 MHz): δ 8.98 (d, 3H), 8.07 (t, 3H), 7.63 (t, 3H), 7.54 (d, 3H), 4.16 (s, 6H), −1.52 (SH, s, 1H). ^{13}C NMR (CD_3CN, 150 MHz): δ 155.2, 148.8, 141.1, 125.0, 124.6, 56.4. IR (ATR, cm^{-1}): 3454, 3067, 2981, 1609, 1575, 1484, 1437, 1374, 1315, 1294, 1268, 1160, 1049, 1021, 906, 839, 765, 733. HRMS (ESI, Pos) calculated for $[C_{18}H_{19}N_4SZn]^+$: 387.0616 found 387.0619. *Anal.* Calc. for $C_{18}H_{19}ZnBF_4N_4S$: C, 45.45; H, 4.03; N, 11.78. Found: C, 45.28; H, 4.09; N, 11.67%.

2.2.8. Preparation of [(TPA)ZnSH]ClO_4, (**8**)

2.2.8.1. Method A. To a solution of [(TPA)ZnSC(O)OMe]ClO_4 (**3**) (120 mg, 0.22 mmol) dissolved in acetonitrile (30 mL) was added 80 μL of water (4.44 mmol, 20 equiv.). The reaction was allowed to stir for 1 week. The acetonitrile solution was then concentrated and addition of diethyl ether (20 mL) resulted in a white solid. The solid was collected, washed with diethyl ether (5 mL) and dried under vacuum to give **8** (50 mg, 47%). ^{1}H NMR (CD_3CN, 600 MHz): δ 8.99 (d, 3H), 8.06 (t, 3H), 7.63 (t, 3H), 7.54 (d, 3H), 4.15 (s, 6H), -1.52 (SH, s, 1H). ^{13}C NMR (CD_3CN, 150 MHz): δ 155.1, 148.8, 141.1, 125.0, 124.6, 56.4. IR (ATR, cm^{-1}): 3071, 2915, 2020, 1608, 1575, 1484, 1437, 1371, 1316, 1296, 1270, 1160, 1076, 1053, 1021, 981, 908, 838, 766, 733. HRMS (ESI, Pos) calculated for $[C_{18}H_{19}N_4SZn]^+$: 387.0616 found 387.0615. *Anal.* Calc. for $C_{18}H_{19}ZnClN_4O_4S$: C, 44.27; H, 3.92; N, 11.47. Found: C, 44.01; H, 3.92; N, 11.29%.

2.2.8.2. Method B. To a solution of tris(2-pyridylmethyl)amine (250 mg, 0.86 mmol) dissolved in dry acetonitrile (6 mL) was added $Zn(ClO_4)_2{\cdot}6H_2O$ (0.32 g, 0.86 mmol). $(CH_3)_4NOH{\cdot}5H_2O$ (156 mg, 0.86 mmol) was then added and the headspace gases

were removed by vacuum. After stirring for 15 min, COS was then bubbled through the solution and the reaction was allowed to stir under a COS atmosphere for 24 h at room temperature. The solution was filtered and the filtrate solvent was concentrated (5 mL) and addition of diethyl ether (20 mL) resulted in a pale yellow solid. The solid was collected, washed with diethyl ether (4 mL) and dried under vacuum to give **8** (310 mg, 73%). The ^{1}H and ^{13}C NMR spectra are identical to the spectra of **8** generated from Method A.

2.2.8.3. Method C. To a solution of tris(2-pyridylmethyl)amine (300 mg, 1.03 mmol) dissolved in dry acetonitrile (40 mL) was added $Zn(ClO_4)_2{\cdot}6H_2O$ (384 mg, 1.03 mmol). After the addition of KOH (58 mg, 1.03 mmol), the headspace gases were removed by vacuum. Hydrogen sulfide was then bubbled through the solution and the reaction was allowed to stir under a H_2S atmosphere for 24 h at room temperature, during which time a white precipitate formed. The solid was collected and extracted with dichloromethane (2×10 mL). The dichloromethane solution was concentrated (5 mL) and addition of diethyl ether (15 mL) resulted in a white solid. The solid was collected, washed with diethyl ether (5 mL) and dried under vacuum to give **8** (150 mg, 30%). The ^{1}H and ^{13}C NMR spectra are identical to the spectra of **8** generated from Method A.

*2.2.9. General procedure used to determine hydrolytic stability of **1**–**6** via ^{1}H NMR*

Water (10–25 equiv.) was added to an NMR tube containing the appropriate thiocarbonate or dithiocarbonate complex (**1**–**6**, typically 4–25 mg) in CD_3CN (0.75 mL). An NMR spectrum was obtained immediately upon mixing and then every 24 h for eight days. For complexes **1**, **5** and **6**, the spectra were unchanged after 8 days, indicating that **1**, **5** and **6** are stable towards hydrolysis at room temperature. For **2**, **3** and **4**, quantitative conversion to **7** or **8** (the hydrolysis product formed depends on the counterion of the original thiocarbonate complex) was observed within 48 h.

*2.2.10. Preparation of $[(TPA)_2Cd](ClO_4)_2$, (**9**)*

To a solution of tris(2-pyridylmethyl)amine (250 mg, 0.86 mmol) dissolved in dry acetonitrile (30 mL) was added $Cd(ClO_4)_2{\cdot}6H_2O$ (360 mg, 0.86 mmol) followed by $(CH_3)_4NOH{\cdot}5H_2O$ (156 mg, 0.86 mmol). After stirring for 15 min, CS_2 (66 mg, 0.85 mmol) was then added to the solution and the reaction was allowed to stir for 24 h at room temperature, during which an insoluble bright yellow precipitate formed. The solution was filtered and the filtrate was concentrated (5 mL) and addition of diethyl ether (20 mL) resulted in a pale yellow solid. The solid was collected, washed with diethyl ether (4 mL) and dried under vacuum to give **9** (330 mg, 87%). Colorless crystals suitable for crystallographic characterization were obtained by diethyl ether diffusion into methanol at room temperature. ^{1}H NMR (CD_3CN, 600 MHz): δ 7.76 (t, 3H), 7.51 (d, 3H), 7.46 (d, 3H), 6.87 (t, 3H), 4.32 (s, 6H). ^{13}C NMR (CD_3CN, 150 MHz): δ 155.1, 148.4, 138.9, 124.5, 123.8, 57.5. IR (ATR, cm^{-1}): 2850, 2017, 1602, 1575, 1480, 1436, 1375, 1308, 1288, 1261, 1218, 1153, 1079, 1052, 1007, 984, 962, 908, 837, 774, 759, 737. A similar reaction using COS instead of CS_2 results in formation of **9** but in a 24% yield.

*2.2.11. Reaction of **8** with CH_3I to form $[(TPA)ZnI]ClO_4$, (**10**)*

To a solution of **8** (50 mg, 0.10 mmol) dissolved in dry acetonitrile (15 mL) was added 5 equiv. of CH_3I (32 μL, 0.51 mmol). The solution was stirred for 10 days at room temperature to ensure complete conversion to product. The solvent was then removed under reduced pressure leaving a white residue. Diethyl ether (2×10 mL) was added and the solid was triturated into a fine crystalline powder. The powder was collected and dried under vacuum (45 mg, 78%). Colorless crystals suitable for crystallographic characterization were obtained by diethyl ether diffusion into acetonitrile at room temperature. The unit cell parameters are identical to the structure of $[(TPA)ZnI]ClO_4$ reported by Canary and co-workers [19]. ^{1}H NMR (CD_3CN, 600 MHz): δ 9.26 (d, 3H), 8.08 (t, 3H), 7.69 (t, 3H), 7.57 (d, 3H), 4.20 (s, 6H). ^{13}C NMR (CD_3CN, 150 MHz): δ 155.0, 149.4, 141.6, 125.0, 124.9, 56.4. IR (ATR, cm^{-1}): 3725, 3704, 3633, 3030, 2010, 1610, 1574, 1483, 1437, 1369, 1316, 1297, 1272, 1227, 1159, 1129, 1077, 1054, 1023, 1001, 980, 966, 908, 896, 837, 780, 762, 731.

*2.2.12. Reaction of **8** with ^{n}BuLi to form $[(TPA)LiClO_4]$, (**11**)*

To a stirred solution of **8** (100 mg, 0.20 mmol) dissolved in dry acetonitrile (15 mL) at −70 °C, 10.0 equiv. of ^{n}BuLi (0.33 mL, 1.6 M in hexanes) was added dropwise. The resulting cloudy mixture was allowed to slowly warm to room temperature and stirred for 24 h. The solvent was then removed under reduced pressure and the residue extracted with dichloromethane (10 mL) and filtered through Celite. The volume was reduced (∼3 mL) and addition of diethyl ether (5 mL) caused the formation of a white solid. The solid was collected, washed with diethyl ether (3 mL) and dried under vacuum (45 mg, 57%). Colorless crystals suitable for crystallographic characterization were obtained by diethyl ether diffusion into dichloromethane at room temperature. ^{1}H NMR (CD_3CN, 600 MHz): δ 8.70 (d, 3H), 7.83 (t, 3H), 7.37 (m, 6H), 3.90 (s, 6H). ^{13}C NMR (CD_3CN, 150 MHz): δ 158.7, 149.4, 138.2, 123.2, 123.2, 58.0. IR (ATR, cm^{-1}): 3366, 3028, 2877, 2846, 2191, 1991, 1643, 1600, 1573, 1480, 1431, 1375, 1316, 1297, 1274, 1212, 1155, 1135, 1108, 1096, 1067, 1048, 1008, 975, 958, 937, 902, 831, 761. *Anal.* Calc. for $C_{18}H_{18}LiClN_4O_4$: C, 54.49; H, 4.57; N, 14.12. Found: C, 54.83; H, 4.73; N, 14.56%.

*2.2.13. Reaction of **8** with NaH to form $[Na_2(TPA)_2(ClO_4)_2]$, (**12**)*

To a stirred solution of **8** (100 mg, 0.20 mmol) dissolved in dry acetonitrile (15 mL), 20 equiv. of NaH (100 mg, 4.0 mmol) was added. The resulting cloudy mixture was stirred for 24 h at room temperature. The solution was filtered and the solvent was removed under reduced pressure. The residue was then extracted with dichloromethane (12 mL) and filtered through Celite. The volume was reduced (∼3 mL) and addition of diethyl ether (8 mL) caused the formation of a white solid. The solid was collected, washed with diethyl ether (3 mL) and dried under vacuum (40 mg, 48%). Colorless crystals suitable for crystallographic characterization were obtained by diethyl ether diffusion into dichloromethane at room temperature. ^{1}H NMR (CD_3CN, 600 MHz): δ 8.59 (d, 3H), 7.73 (t, 3H), 7.32 (t, 3H), 7.26 (d, 3H), 3.76 (s, 6H). ^{13}C NMR (CD_3CN, 150 MHz): δ 158.2, 149.9, 137.2, 123.7, 122.6, 59.3. IR (ATR, cm^{-1}): 3841, 3753, 3675, 3651, 3616, 2846, 1597, 1571, 1479, 1437, 1371, 1315, 1300, 1270, 1215, 1156, 1095, 1062, 1048, 1004, 989, 977, 959, 926, 903, 835, 764. *Anal.* Calc. for $C_{36}H_{36}Na_2Cl_2N_8O_8$: C, 52.37; H, 4.40; N, 13.57. Found: C, 52.65; H, 4.48; N, 13.51%.

2.3. X-ray crystallography

Suitable crystals were obtained from slow vapor diffusion and mounted on a glass fiber using hydrocarbon oil and cooled under a nitrogen stream to 150(1) K. A Nonius Kappa CCD diffractometer (Mo Kα radiation; λ = 0.71073 Å) was used for data collection. Unit cell parameters were determined from 10 data frames with an oscillation range of 1°/frame and an exposure time of 20 s/frame. Indexing and unit cell refinement based on the reflections from the initial set of frames were consistent with monoclinic *P* lattices for **7**, **9**, **11** and **12**, triclinic *P* lattices for **1** and **5**, an orthorhombic *P* lattice for **2** and a tetragonal *P* lattice for **6**. The intensity data for each compound was then collected. These reflections were then indexed, integrated and corrected for Lorentz, polarization and absorption effects using DENZO-SMN and SCALEPAC [20]. The

space group for each compound was determined from the systematic absences in the diffraction data. The structures were solved by a combination of direct and heavy atom methods using SIR 97 [21]. Compound **2** contains a BF_4 anion disordered over two positions with an 83:17 occupancy ratio. Compound **5** contains two crystallographically independent molecules per unit cell. Compound **6** contains a CH_3OH molecule that is within H-bonding distance of atom O1 of **6**. Compound **7** contains two crystallographically independent molecules and one molecule of THF per asymmetric unit. Compound **12** contains a disordered perchlorate anion with a 64:36 occupancy ratio. Compounds **1**, **9** and **11** contained only one molecule per asymmetric unit, no co-crystallized solvent and no positional disorder. All non-hydrogen atoms were refined with anisotropic displacement parameters. All hydrogen atoms were placed in ideal positions and assigned isotropic displacement coefficients $U(H) = 1.2\ U(C)$ or $1.5\ U(C_{methyl})$ and allowed to ride on their respective carbons using SHELXL-97 [22]. A summary of the crystallographic data and parameters for **1**, **2**, **5**, **6** and **7** are found in Table 1 and for **9**, **11** and **12** in Table S1.

2.4. Computational methods

All calculations were carried out using GAUSSIAN 03 [23]. Geometry optimizations were carried out using the 6-311 + G(d,p) basis set for all atoms, except for Zn, for which the Stuttgart effective core potential basis set was used [24]. Among various density functionals considered here, TPSSH [25] was chosen as the functional for geometric and electronic analysis given that gas phase optimization with TPSSH was best able to reproduce geometries from crystal structures for the TpZn–SH [12] and $[(TPA)Zn–SH]^+$ complexes (Table S2). Geometries were also optimized in acetonitrile solvent with TPSSH using the IEF-PCM implicit solvent model. Wiberg bond indices and natural population analysis (NPA) charges were computed using the NBO 3.1 program [26]. For the purpose of calculating Mulliken charge populations and Fukui nucleophilicity indices, calculations were carried out with the more balanced 6-31G(d,p) basis set (except again using the Stuttgart effective core potential basis set for Zn), which has been used successfully to this end in related studies [27,28]. The Fukui nucleophilicity index for an atom has been calculated using the N-electron equilibrium geometry and taking the difference in Mulliken charge population for the atom in the N-electron and (N-1)-electron cases [29].

3. Results and discussion

3.1. Synthesis of alkyl thiocarbonate and dithiocarbonate complexes 1–6

Our aim was to prepare $[(TPA)M–SH]^+$ complexes (where M = Zn or Cd) via insertion of COS or CS_2 into the metal hydroxide bond followed by elimination of CO_2 or COS to give the cationic metal hydrosulfide complexes. Instead, the formation of *O*-alkyl thiocarbonate and dithiocarbonate complexes was observed. $[(TPA)Zn–SC(S)OCH_3]ClO_4$ (**1**), $[(TPA)Zn–SC(O)OCH_3]BF_4$ (**2**), $[(TPA)Zn–SC(O)OCH_3]ClO_4$ (**3**), $[(TPA)Zn–SC(O)OCH_2CH_3]BF_4$ (**4**), $[(TPA)Cd–SC(S)OCH_3]ClO_4$ (**5**) and $[(TPA)Cd–SC(O)OCH_3]ClO_4$ (**6**) were synthesized in 27–75% yield using the synthetic route outlined in Scheme 2. The compounds were obtained by the reaction of equimolar amounts of TPA, the appropriate metal salt, and KOH in either dry methanol or ethanol followed by bubbling of COS or addition of CS_2. Compounds **1**–**6** were characterized by ^1H and ^{13}C NMR, IR, elemental analysis (CHN) and, for **1**, **2**, **5** and **6**, by single-crystal X-ray crystallography. One possible mechanism for formation of products **1**–**6** could be the esterification of $[(TPA)M–SC(E)OH]^+$ (M = Zn, Cd; E = O, S) by the protic solvent (MeOH or EtOH), where $[(TPA)M–SC(E)OH]^+$ is the product initially formed after heterocumulene insertion into the M-OH bond. However, we cannot rule out the possibility that **1**–**6** may result from heterocumulene insertion into an M-OR (R = alkyl group) rather than an M-OH bond. Trace amounts of a metal alkoxide species may be in equilibrium with the metal hydroxide in alcoholic solvents, as observed with the $Tp^{R,Me}$ systems [30].

The spectroscopic data for complexes **1**–**6** are very similar, supporting the assignment that complexes **3** and **4**, for which crystals

Table 1
Summary of X-ray crystallographic data and parameters.[a]

	1	**2**	**5**	**6**·CH_3OH	**7**·THF
Formula	$C_{20}H_{21}ZnClN_4O_5S_2$	$C_{20}H_{21}ZnBF_4N_4O_2S$	$C_{20}H_{21}CdClN_4O_5S_2$	$C_{21}H_{25}CdClN_4O_7S$	$C_{40}H_{46}Zn_2B_2F_8N_8S_2$
Formula weight	562.35	533.69	609.38	625.36	1023.33
Crystal system	triclinic	orthorhombic	triclinic	tetragonal	monoclinic
Space group	$P\bar{1}$	***P**bca*	$P\bar{1}$	$\boldsymbol{P}4_1$	$\boldsymbol{P}2_1/n$
a (Å)	9.01650(10)	15.7630(3)	12.41510(10)	12.15630(10)	12.0202(6)
b (Å)	10.47920(10)	13.9487(2)	14.3038(2)	12.15630(10)	13.5953(6)
c (Å)	13.2119(2)	20.4444(4)	14.8828(2)	17.20910(10)	27.6430(14)
α (°)	105.7602(5)	90	62.8664(5)	90	90
β (°)	102.4322(6)	90	87.4922(7)	90	97.3819(19)
γ (°)	97.5275(7)	90	84.3322(7)	90	90
V (Å^3)	1149.14(2)	4495.18(14)	2340.57(5)	2543.09	4479.9(4)
Z	2	8	4	4	4
D_{calc} (Mg m^{-3})	1.625	1.577	1.729	1.633	1.517
T (K)	150(1)	150(1)	150(1)	150(1)	150(1)
Color	colorless	colorless	colorless	yellow	colorless
Crystal size (mm)	0.35 × 0.30 × 0.25	0.25 × 0.23 × 0.15	0.35 × 0.25 × 0.20	0.25 × 0.18 × 0.10	0.28 × 0.13 × 0.03
Absorption coefficient (mm^{-1})	1.407	1.244	1.266	1.094	1.240
θ range (°)	1.66–27.89	2.79–27.49	1.64–27.50	2.65–27.47	1.77–26.39
Completeness to θ (%)	99.5	99.8	99.6	99.9	95.4
Reflections collected	10230	9745	20151	5732	13461
Independent reflections	5450	5147	10712	5732	8340
Parameters	383	318	595	313	569
R_1/wR_2 (all data)[b]	0.0296/0.0648	0.0562/0.0875	0.0298/0.0603	0.0232/0.0471	0.1336/0.1275
Goodness-of-fit	1.034	1.044	1.068	1.094	1.020
Difference in peak/hole (e/Å^{-3})	0.588/−0.437	0.414/−0.423	0.665/−0.635	0.575/−0.338	0.552/−0.488

[a] Radiation used: Mo Kα (λ = 0.71073 Å).
[b] $R_1 = S||F_o| - |F_c||/S|F_o|$; $wR_2 = [S[w(F_o^2 - F_c^2)^2]/[S(F_o^2)^2]]^{1/2}$, where $w = 1/[s^2(F_o^2) + (aP)^2 + bP]$.

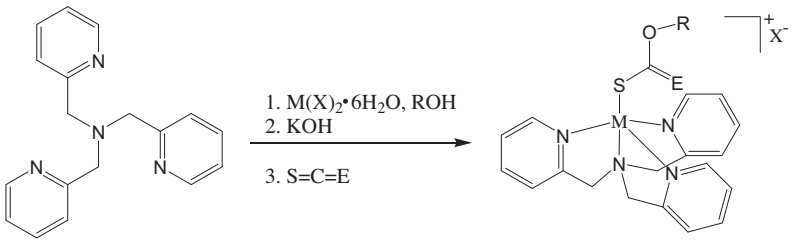

*1 M = Zn, E = S, R = CH_3, X = ClO_4
*2 M = Zn, E = O, R = CH_3, X = BF_4
3 M = Zn, E = O, R = CH_3, X = ClO_4
4 M = Zn, E = O, R = CH_2CH_3, X = BF_4
*5 M = Cd, E = S, R = CH_3, X = ClO_4
*6 M = Cd, E = O, R = CH_3, X = ClO_4

Scheme 2. Zn(II) and Cd(II) alkyl dithiocarbonate and thiocarbonate complexes **1**–**6**. Asterisks indicate those complexes characterized by X-ray diffraction.

suitable for X-ray crystallography have not been obtained, have atom sequences similar to complexes **1**, **2**, **5** and **6**. Particularly diagnostic in the ^1H and ^{13}C NMR is the observation of the -OCH_3 resonances for **1**–**3** and **5**–**6** and the –OCH_2CH_3 resonances for **4**. Evidence for the thiocarbonate group in complexes **2**–**4** and **6** and the dithiocarbonate group in complexes **1** and **5** is provided by ^{13}C NMR, with the observation of carbon resonances at ~177 ppm and 228 ppm, respectively. In the FTIR, a band at ~1645 cm^{-1} was assigned as the C=O vibration of the thiocarbonate ligand for complexes **2**–**4** and **6**. However, the C=S vibration for the dithiocarbonate ligand was not observed in complexes **1** and **5** due to overlapping vibrations associated with the ClO_4^- and BF_4^- anions.

3.2. X-ray structures of complexes *1*, *2*, *5* and *6*

The molecular structures of [(TPA)Zn–SC(S)OCH_3]ClO_4 (**1**) and [(TPA)Zn–SC(O)OCH_3]BF_4 (**2**) are shown in Figs. 1 and 2. A summary of the X-ray crystallographic data and refinement parameters for the two complexes is provided in Table 1. Complexes **1** and **2** are monomeric and the zinc ion in each complex is coordinated by four nitrogen atoms from the TPA ligand and a sulfur atom from either an *O*-methyl dithiocarbonate or *O*-methyl thiocarbonate ligand. The dithiocarbonate and thiocarbonate ligands in **1** and **2** are oriented such that the more sterically demanding –OCH_3 unit of the ligands is pointed away from zinc. The coordination environment around the zinc ion in each complex can be described as distorted trigonal bipyramidal. The tertiary amine nitrogen atom of the TPA ligand and the sulfur atom of the dithiocarbonate ligand in **1** or thiocarbonate ligand in **2** occupy the axial positions. The τ_5 values of 0.83 for **1** and 0.89 for **2** (where $\tau_5 = 0$ is expected for an idealized square pyramidal geometry and $\tau_5 = 1.0$ for an idealized trigonal bipyramidal geometry [31]) are similar and indicate the same degree of distortion from an idealized trigonal bipyramidal geometry. Surprisingly, a search of the Cambridge Structural Database for a complex containing the fragment M-SC(O)OR where M = Zn or Cd resulted in no structures. However, examples of metal complexes, besides Zn or Cd complexes, containing an alkyl thiocarbonate group have been reported [32].

The binding mode of the dithiocarbonate and thiocarbonate ligands in **1** and **2** can be described as monodentate. In **1**, the Zn1–S1 and Zn1···S2 distances are 2.3590(4) and 3.2994(5) Å, while in **2**, the Zn1–S1 and Zn1···O1 distances are 2.3332(5) and 3.273(16) Å. The Zn1···S2 distance in **1** and Zn1···O1 distance in **2** are clearly too long for any type of interaction. The S1–Zn1–N2 bond angles in **1** and **2** are almost linear (175.30(3)° for **1** and 172.98(4)° for **2**) consistent with monodentate binding modes for the dithiocarbonate and thiocarbonate ligands. The Zn–S distances are similar between the two complexes (2.3590(4) Å in **1** and 2.3332(5) Å in **2**) and compare well with other five-coordinate zinc complexes [33]. However, the Zn–S distance in both complexes is significantly longer when compared to the values of four-coordinate $Tp^{Ph,Me}$Zn–SC(S)OR′ complexes (when R′ = Et, 2.264 Å; R′ = Me, 2.244 Å) [30b,34].

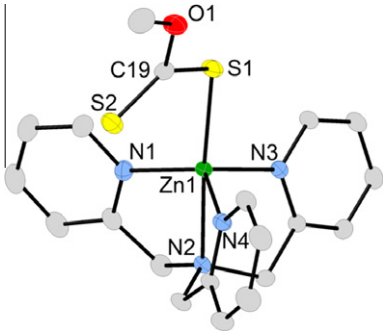

Fig. 1. Representation of the cationic portion of the X-ray structure of **1** with thermal ellipsoids drawn at 50% probability level and hydrogen atoms omitted for clarity. Important bond lengths (Å): Zn1–S1 2.3590(4), Zn1···S2 3.2994(5), Zn1–N1 2.0790(13), Zn1–N2 2.2685(13), Zn1–N3 2.1142(13), Zn1–N4 2.0805(13), S1–C19 1.7325(17), S2–C19 1.6544(17). Bond angles (°): S1–Zn1–N1 104.62(4), S1–Zn1–N2 175.30(3), S1–Zn1–N3 97.88(4), S1–Zn1–N4 105.09(4), N1–Zn1–N2 77.40(5), N1–Zn1–N3 110.54(5), N1–Zn1–N4 125.29(5), N2–Zn1–N3 77.42(5), N2–Zn1–N4 76.67(5), N3–Zn1–N4 109.53(5), C19–S1–Zn1 99.91(6), S2–C19–S1 125.55(10).

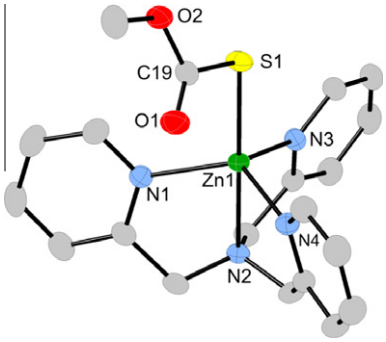

Fig. 2. Representation of the cationic portion of the X-ray structure of **2** with thermal ellipsoids drawn at 50% probability level and hydrogen atoms omitted for clarity. Important bond lengths (Å): Zn1–S1 2.3332(5), Zn1···O1 3.273(16), Zn1–N1 2.1065(16), Zn1–N2 2.2630(16), Zn1–N3 2.1005(16), Zn1–N4 2.0700(16), S1–C19 1.744(2), O1–C19 1.206(3). Bond angles (°): S1–Zn1–N1 102.58(5), S1–Zn1–N2 172.98(4), S1–Zn1–N3 97.36(5), S1–Zn1–N4 108.38(5), N1–Zn1–N2 76.64(6), N1–Zn1–N3 115.14(6), N1–Zn1–N4 119.88(6), N2–Zn1–N3 76.91(6), N2–Zn1–N4 77.70(6), N3–Zn1–N4 110.37(6), C19–S1–Zn1 100.99(7), O1–C19–S1 127.14(17).

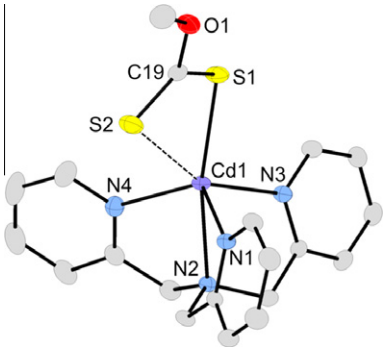

Fig. 3. Representation of the cationic portion of the X-ray structure of **5** with thermal ellipsoids drawn at 50% probability level and hydrogen atoms omitted for clarity. Important bond lengths (Å): Cd1–S1 2.5160(5), Cd1–S2 3.0535(5), Cd1–N1 2.2969(15), Cd1–N2 2.4268(14), Cd1–N3 2.3934(15), Cd1–N4 2.3199(16), S1–C19 1.7222(19), S2–C19 1.6641(19). Bond angles (°): S1–Cd1–N1 116.95(4), S1–Cd1–N2 163.13(4), S1–Cd1–N3 93.07(4), S1–Cd1–N4 113.48(4), N1–Cd1–N2 71.15(5), N1–Cd1–N3 102.92(5), N1–Cd1–N4 116.49(5), N2–Cd1–N3 70.29(5), N2–Cd1–N4 71.70(5), N3–Cd1–N4 110.38(5), C19–S1–Cd1 92.18(6), S2–C19–S1 124.95(11).

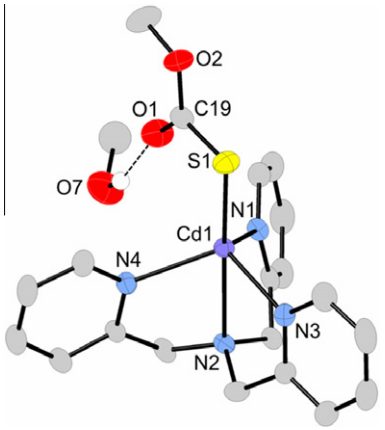

Fig. 4. Representation of the cationic portion of the X-ray structure of **6** with thermal ellipsoids drawn at 50% probability level and hydrogen atoms (except the hydrogen on O7) are omitted for clarity. Important bond lengths (Å): Cd1–S1 2.4715(6), Cd1··O1 2.978(2), Cd1–N1 2.2955(18), Cd1–N2 2.4191(18), Cd1–N3 2.3301(18), Cd1–N4 2.3203(19), S1–C19 1.733(3), O1–C19 1.214(3), O2–C19 1.348(3). Bond angles (°): S1–Cd1–N1 117.06(5), S1–Cd1–N2 168.68(5), S1–Cd1–N3 98.60(5), S1–Cd1–N4 107.19(5), N1–Cd1–N2 73.06(7), N1–Cd1–N3 113.09(7), N1–Cd1–N4 109.84(7), N2–Cd1–N3 71.72(7), N2–Cd1–N4 71.97(7), N3–Cd1–N4 110.46(7), C19–S1–Cd1 92.89(8), O1–C19–S1 126.08(19).

The molecular structures of $[(TPA)Cd–SC(S)OCH_3]ClO_4$ (**5**) and $[(TPA)Cd–SC(O)OCH_3]ClO_4$ (**6**), which are the cadmium analogs of **1** and **2**, were also determined by X-ray crystallography. Their structures are shown in Figs. 3 and 4 and their crystallographic data and refinement parameters are listed in Table 1. When compared to **1** and **2**, the structures of **5** and **6** are similar but differences do exist between the zinc and cadmium analogs. For instance, the dithiocarbonate ligand in **1** is monodenate but in **5** the dithiocarbonate ligand could be classified as weakly anisobidentate. The two Cd–S distances of the dithiocarbonate ligand are 2.5160(5) and 3.0535(5) Å. The Cd1···S2 distance (3.0535(5) Å) is longer than the sum of the covalent radii (2.56 Å), but significantly shorter than the sum of the van der Waals radii (3.38 Å), indicative of a weak interaction. The S1–Cd1–N2 angle (163.13(4)°) in **5** compared to the S1–Zn1–N2 angle in **1** (175.30(3)°) is also considerably smaller. The smaller S1–M–N2 (M = Zn or Cd) angle in **5** illustrates how the large cadmium atom has adjusted for the Cd1···S2 interaction at the expense of the S1–Cd1–N2 angle.

Fig. 4 shows the structure for $[(TPA)Cd–SC(O)OCH_3]ClO_4$ (**6**). Complex **6** is, to the best of our knowledge, the first structurally characterized cadmium complex containing an *O*-alkyl thiocarbonate ligand. The geometry of the cadmium center is distorted trigonal bipyramidal ($\tau_5 = 0.86$), where three pyridine nitrogen atoms (N2, N3 and N4) make up the equatorial positions and N2 and S1 the axial positions. In addition, a methanol molecule is hydrogen bonded to O1 of the thiocarbonate ligand. The Cd ion in **6** is located 0.69 Å (compared to 0.76 Å for **5**) above the equatorial plane defined by the three pyridine nitrogen atoms, which is significantly farther than the Zn ion in **1** and **2** (~0.47 Å). The Cd1–S1 and Cd1···O1 distances of the thiocarbonate ligand are 2.4715(6) and 2.978(2) Å, respectively. The Cd1···O1 distance is approximately the same as the van der Waals distance (3.10 Å) indicating the thiocarbonate ligand in **6**, similar to **2**, has a monodentate coordination mode. The Cd1–S1 distance (2.4715(6) Å) is shorter than the Cd1–S1 distance (2.5160(5) Å) in **5** but is similar to Cd–S distances observed in cadmium complexes with thiolate ligands (2.47–2.55 Å) [35] but shorter than cadmium complexes with bidendate alkyl dithiocarbonate ligands (2.65–2.86 Å) [33a].

3.3. Synthesis of cationic zinc hydrosulfide complexes

Three general routes to cationic zinc and cadmium hydrosulfide complexes of the form $[(TPA)M–SH]^+$ (M = Zn or Cd) were explored (Scheme 3) [14]. Of these routes, methods A and B represent new methods for making Zn–SH complexes, while method C has been used to make TpZn–SH complexes [12] but not cationic $[LZn–SH]^+$ (where L = ligand) complexes.

Method A investigated the hydrolytic stability of complexes **1**–**6** towards water. Prior studies by Vahrenkamp had shown that $Tp^{tBu,Me}Zn–OC(O)OR$ complexes are easily hydrolyzed to $Tp^{tBu,Me}Zn–OH$ [36]. Interestingly, the related $Tp^{Cum,Me}Zn–OC(O)OR$ complexes are stable in water/alcohol mixtures, suggesting the more encapsulating $Tp^{Cum,Me}$ ligand is responsible for the increased stability [5]. The stability of complexes **1**–**6** towards hydrolysis was initially examined by ^1H NMR. Treatment of **2**, **3** and **4** in CD_3CN with water results in the quantitative formation of [(TPA)Zn–SH]X (X = BF_4^- (**7**) and ClO_4^- (**8**)) within 48 h. The hydrolysis of **3** on a preparative scale yielded **8** in a 47% yield. A detailed description of the characterization of **7** and **8**, including the X-ray structure of **7**, follows in the next section. Interestingly, under the same conditions, **1**, **5** and **6** show no signs of hydrolysis, even after 8 days.

Method B involves the reaction of equimolar amounts of TPA, $M(ClO_4)_2·6H_2O$ and $Me_4NOH·5H_2O$ with COS or CS_2 in CH_3CN. This procedure is similar to the procedure used to make **1**–**6** except the protic solvent (MeOH or EtOH) and KOH have been replaced with CH_3CN and $Me_4NOH·5H_2O$ ($Me_4NOH·5H_2O$ was used as the base because of the poor solubility of KOH in acetonitrile). The rationale for switching the solvent to acetonitrile was to prevent incorporation of the solvent into the products, as was observed with the formation of **1**–**6** in alcoholic solutions. Treatment of TPA, $Zn(ClO_4)_2·6H_2O$ and $Me_4NOH·5H_2O$ with COS yielded $[(TPA)Zn–SH]ClO_4$ (**8**) in a 73% yield. Surprisingly, replacing COS with CS_2, under the same reaction conditions, does not result in a zinc hydrosulfide (as evidenced by the absence of a SH resonance in the ^1H NMR) but an unidentified mixture of products.

The reaction was also run using $Cd(ClO_4)_2·6H_2O$ but, rather than isolating a cadmium hydrosulfide, an insoluble yellow precipitate (presumably CdS) and a soluble species containing only TPA resonances in the ^1H NMR were obtained. X-ray crystallography identified the soluble species as $[(TPA)_2Cd](ClO_4)_2$ (**9**), resulting from ligand redistribution (see Fig. S1 for structure of **9**). The structure of **9** has been reported by Bebout [37]. However, the structure of

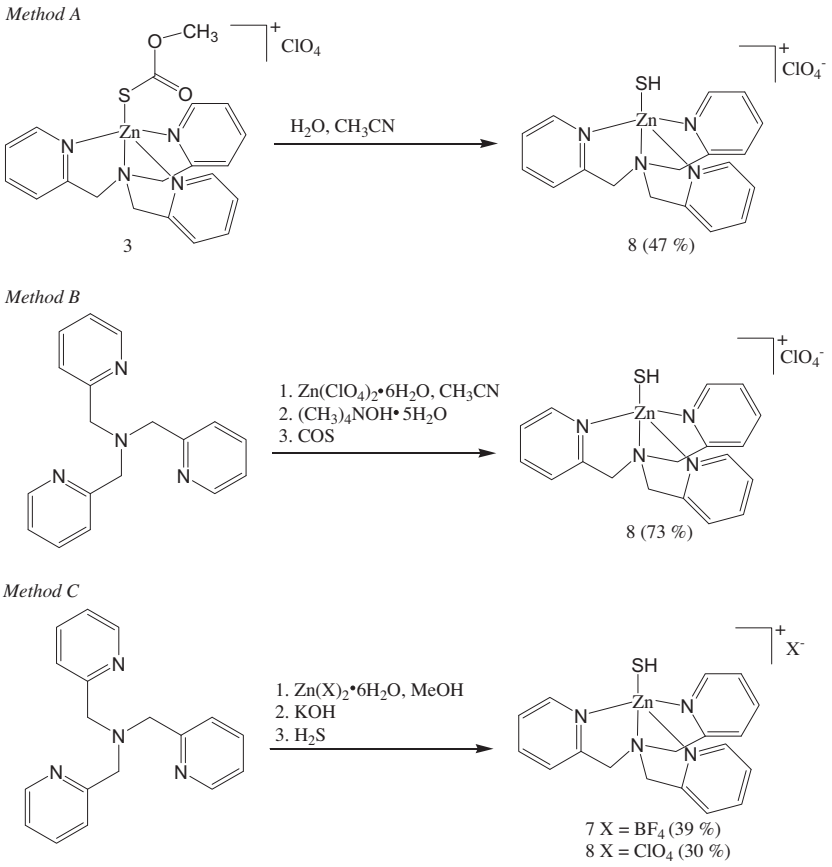

Scheme 3. Different methods for preparing $[(TPA)Zn–SH]^+$ complexes. Yields are for preparative scale reactions.

9 obtained by Bebout et al. crystallized in a different space group ($P\bar{1}$), as a result of a co-crystallized toluene molecule.

Method C explored the direct method of treating the cadmium and zinc hydroxide complexes with H_2S. This procedure is used to make $Tp^{R,Me}Zn–SH$ complexes from $Tp^{R,Me}Zn–OH$ [5]. Bubbling of H_2S through a CH_3OH solution of $[((TPA)Zn)_2(\mu\text{-}OH)_2](X)_2$ (where $X = BF_4^-$ or ClO_4^-) led to the formation of **7** and **8** in a 39% and 30% yield, respectively. Repeated attempts to make a cadmium hydrosulfide from $[((TPA)Cd)_2(\mu\text{-}OH)_2](ClO_4)_2$ and H_2S always resulted in insoluble CdS.

3.4. Characterization of $[(TPA)Zn–SH]^+$ complexes 7 and 8

Complexes $[(TPA)Zn–SH]BF_4$ (**7**) and $[(TPA)Zn\text{-}SH]ClO_4$ (**8**) were characterized by ^1H and ^{13}C NMR, IR, elemental analysis (CHN), electrospray mass spectrometry (ESI-MS) and, for **7**, by X-ray crystallography. The compounds are stable in acetonitrile but begin to decompose within one day after dissolution in chloroform. The spectroscopic data for complexes **7** and **8** are identical, supporting the claim that **8** is similar in structure to **7**. In the ^1H and ^{13}C NMR, the three pyridyl groups in both complexes are equivalent, indicative of tridentate coordination of the TPA ligand to the zinc center. The SH resonance for **7** and **8** is observed in CD_3CN as a singlet at −1.5 ppm. Exchange of this resonance with deuterium occurs with D_2O or CD_3OD, consistent with the assignment of the −1.5 ppm resonance as the SH proton. The ^1H NMR chemical shift value for the SH proton in **7** and **8** also falls within the range (−2.1 to −1.0 ppm) observed by the zinc hydrosulfide complexes $Tp^{R,Me}Zn–SH$ (R = phenyl, 3-pyridyl, 4-picolyl and t-butyl) [12]. The IR spectra of **7** and **8** did not show a ν(SH) vibration.

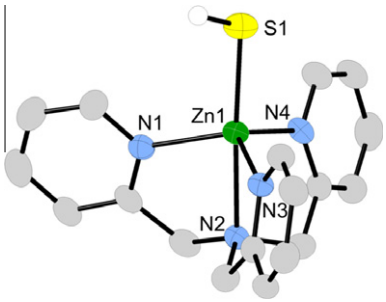

Fig. 5. Representation of the cationic portion of the X-ray structure of $[(TPA)Zn–SH]BF_4$ (**7**) with thermal ellipsoids drawn at 50% probability level and hydrogen atoms (with the exception of the S–H hydrogen atom) are omitted for clarity. Important bond lengths (Å): Zn1–S1 2.3207(14), Zn1–N1 2.089(4), Zn1–N2 2.308(4), Zn1–N3 2.086(4), Zn1–N4 2.080(4). Bond angles (°): S1–Zn1–N1 106.25(12), S1–Zn1–N2 176.33(10), S1–Zn1–N3 104.39(12), S1–Zn1–N4 100.14(11), N1–Zn1–N2 76.10(15), N1–Zn1–N3 115.46(14), N1–Zn1–N4 110.14(16), N2–Zn1–N3 76.77(15), N2–Zn1–N4 76.31(14), N3–Zn1–N4 118.31(15).

The structure of the cationic portion of $[(TPA)Zn–SH]BF_4$ (**7**) is shown in Fig. 5. The complex is mononuclear and the zinc ion is five-coordinate and displays approximately trigonal bipyramidal geometry. The hydrogen atom of the SH group was not located in the difference Fourier map, but its presence is supported by one tetrafluoroborate anion per cation and by ^1H NMR (singlet at −1.5 ppm). The hydrosulfide and tertiary amine occupy the axial positions, while the three pyridyl rings occupy the equatorial positions. The structure is identical to $[(TPA)Zn–SH]BPh_4$, which has just recently been published [14].

Table 2
Comparison of Zn–SH ligation in the TpZn–SH and $[(TPA)Zn–SH]^+$ complexes.

	TpZn–SH (gas phase)	TpZn–SH (acetonitrile)	$[(TPA)Zn–SH]^+$ (gas phase)	$[(TPA)Zn–SH]^+$ (acetonitrile)
Bond distance (Å)	2.219	2.236	2.280	2.289
Wiberg bond index	0.453	0.447	0.399	0.386

Table 3
Mulliken charge populations computed for Zn and the SH ligand in the TpZn–SH and $[(TPA)Zn–SH]^+$ complexes.

	TpZn–SH (gas phase)	TpZn–SH (acetonitrile)	$[(TPA)Zn–SH]^+$ (gas phase)	$[(TPA)Zn–SH]^+$ (acetonitrile)
Zn	0.411	0.416	0.533	0.549
SH	−0.266	−0.280	−0.303	−0.328
Charge difference	0.678	0.697	0.836	0.877

A comparison of the metrical parameters around the zinc ion between the active site structure of human carbonic anhydrase II (HCA II) bound with anionic hydrogen sulfide (1CAO) [38] and the model complexes $[(TPA)Zn–SH]BF_4$ (**7**) and $Tp^{R,Me}Zn–SH$ (R = phenyl, 3-pyridyl or 4-picolyl) [12] shows important differences and similarities. For instance, the Zn–S distance (2.3207(14) Å) in **7** is significantly longer compared to the Zn–S distance in HCA II (2.2 Å) and $Tp^{R,Me}Zn–SH$ ($Zn–S_{avg}$ = 2.214 Å). The longer Zn–S bond can be attributed to the coordination of the tertiary amino nitrogen of the TPA ligand which elongates the *trans* Zn–SH bond distance. In addition, we would like to note that there are three potential hydrogen bonding interactions to the SH ligand in the 1CAO active site (Thr199 side chain hydroxyl group and crystallized waters HOH338 and HOH218) that may affect how SH ligates to Zn^{2+} in 1CAO. As such, not having such interactions in the TPA and Tp complexes means that the structural comparisons, while interesting, should be considered with this caveat in mind. Finally, the $Zn–N_{pyridine}$ bond distances ($Zn–N_{avg}$ = 2.09 Å) and $S–Zn–N_{pyridine}$ angles ($S–Zn–N_{avg}$ = 103.6°) in **7** are more similar to HCA II ($Zn–N_{avg}$ = 2.13 Å and $S–Zn–N_{avg}$ = 110.8°) compared to $Tp^{R,Me}Zn–SH$ ($Zn–N_{avg}$ = 2.06 Å and $S–Zn–N_{avg}$ = 123.8°).

3.5. Computational comparison between $[(TPA)Zn–SH]^+$ and TpZn–SH

DFT calculations provide evidence for a stronger ligation of hydrosulfide to the zinc center in TpZn–SH than in $[(TPA)Zn–SH]^+$ (Table 2). The Zn–S distance in the former is shorter by 0.061 Å in the gas phase and similarly by 0.053 Å in acetonitrile. This is consistent with the Zn–S Wiberg bond index being 0.054 greater in the Tp complex in the gas phase and 0.061 greater in acetonitrile. Likewise, there is a greater polarity in the Zn–SH bond in the TPA complex. Examination of the Mulliken charge populations on Zn and the hydrosulfide ligand (Table 3) in the two complexes reveals a greater difference in charge between the metal center and SH ligand in the TPA complex versus the Tp complex. This measure of bond polarity shows a small increase in going from the gas phase to acetonitrile solvent. The same trend is observed if NPA charges are considered (Table S3). Finally, Fukui nucleophilicity indices for the hydrosulfide ligand in TpZn–SH and $[(TPA)Zn–SH]^+$ (Table 4) indicate that the SH ligand is more nucleophilic in the Tp complex, consistent with the reactivity trend observed upon methylating the two hydrosulfide complexes with methyl iodide [12].

3.6. Reactivity of $[(TPA)ZnSH]ClO_4$, (**8**)

Preliminary reactivity studies were performed with $[(TPA)Zn–SH]ClO_4$ (**8**) and comparisons were made to the more thoroughly studied $Tp^{R,Me}Zn–SH$ system. Prior studies by Rombach and Vahrenkamp [12] had shown that the zinc-bound hydrosulfide in the $Tp^{Ph,Me}Zn–SH$ system is alkylated by CH_3I to give $Tp^{Ph,Me}ZnI$ and methanethiol. In contrast to $Tp^{Ph,Me}Zn–SH$, the reaction of CH_3I and **8** at room temperature is extremely slow, requiring about 9 days for completion, as evidenced by ^1H NMR. This result is supported by the DFT calculations, which suggest a decreased nucleophilicity for $[(TPA)Zn–SH]^+$ compared to TpZn–SH. Treatment of **8** on a preparative scale in CH_3CN with CH_3I (~5 equiv.) resulted in the isolation of $[(TPA)ZnI]ClO_4$ (**10**) in a 78% yield. The product was identified by ^1H and ^{13}C NMR and X-ray crystallography. Formation of **10** was evident in the ^1H NMR by the absence of the SH resonance present in **8** and the downfield shift of the TPA resonances. Crystals of the product were obtained and gave identical unit cell parameters for $[(TPA)ZnI]ClO_4$, which has been previously characterized by X-ray crystallography [19].

Table 4
Fukui nucleophilicity index for the SH ligand in the TpZn–SH and $[(TPA)Zn–SH]^+$ complexes.

TpZn–SH (gas phase)	$[(TPA)Zn–SH]^+$ (gas phase)
0.742	0.535

Attempts to make an unknown metallothiolate via deprotonation of the hydrosulfide ligand in **8** using *n*-butyllithium and NaH failed. The deprotonation reactions resulted in the elimination of zinc sulfide and formation of the products $[(TPA)LiClO_4]$ (**11**) and $[((TPA)Na)_2(\mu\text{-}ClO_4)_2]$ (**12**), respectively. The composition of **11** and **12** were determined by spectroscopic methods (NMR, IR), elemental analysis and X-ray crystallography. The structures for both complexes are provided in Figs. S2 and S3 in the Supporting information. Compound **11** is monomeric and the lithium ion is bound by the TPA ligand and the perchlorate anion in a trigonal bipyramidal geometry. Conversely, **12** is dimeric with each sodium ion coordinated to a TPA ligand and two bridging perchlorate anions. Interestingly, the $Tp^{Cum,Me}Zn–SH$ reaction with *n*-butyllithium results in SH substitution to form $Tp^{Cum,Me}Zn–C_4H_9$ instead of ZnS elimination [12].

4. Conclusion

The insertion of COS and CS_2 into the M-OH bond of $[((TPA)M)_2(\mu\text{-}OH)_2](ClO_4)_2$ (M = Zn, Cd) in alcoholic media results in *O*-alkyl thiocarbonate and dithiocarbonate zinc and cadmium complexes. These complexes were characterized by spectroscopic methods and, in several cases, by X-ray crystallography. Complexes **2** and **6** represent the first examples of structurally characterized Zn and Cd complexes containing a M-SC(O)OR (M = Zn, Cd and R = alkyl group) fragment. The *O*-alkyl thiocarbonate zinc complexes were determined to be susceptible to hydrolysis resulting

in zinc hydrosulfide complexes of the general formula [(TPA)Zn–SH]$^+$. Several other synthetic routes were also described for making [(TPA)Zn–SH]$^+$ complexes. Furthermore, reactivity and DFT studies comparing cationic [(TPA)Zn–SH]$^+$ with neutral TpZn–SH were conducted and many similarities and differences between the two complexes were found.

Acknowledgements

E.C.B. thanks Boise State University for support of this project and Jeff Habig (Boise State University) for assistance with mass spectrometry. N.G.S. and B.J.I. were supported by a summer fellowship by NIH Grant #P20 RR0116454 from the INBRE Program of the National Center for Research Resources. S.V.K. and B.F.G. were supported by a SURE grant from the College of Natural Sciences and Mathematics at California State University, Sacramento. NMR, FT-IR and ESI-MS were made possible through funds from NSF to Boise State University (CRIF/MU-0639251, CCLI-0737128 and CHE-0923535, respectively).

Appendix A. Supplementary material

Computational details and the molecular structures and crystallographic data and refinement parameters for **9**, **10** and **11** are provided. CCDC 838215, 838216, 838217, 838218, 838219, 838220, 838221, and 838222 contain the supplementary crystallographic data for compounds **1**, **2**, **5**, **6**, **7**, **9**, **11**, and **12**. These data can be obtained free of charge from The Cambridge Crystallographic Data Centre via www.ccdc.cam.ac.uk/data_request/cif. Supplementary data associated with this article can be found, in the online version, at doi:10.1016/j.ica.2012.01.040.

References

[1] (a) W.N. Lipscomb, N. Sträter, Chem. Rev. 96 (1996) 2375;
(b) G. Parkin, Chem. Rev. 104 (2004) 699.
[2] N.U. Meldrum, F.J.W. Roughton, J. Physiol. (Lond.) 80 (1933) 113.
[3] Y. Pocker, S. Sarkanen, in: A. Meister (Ed.), Advances in Enzymology and Related Areas of Molecular Biology, vol. 47, John Wiley & Sons, Inc., Hoboken, NJ, USA, 2006.
[4] J. Notni, S. Schenk, G. Protoschill-Krebs, J. Kesselmeier, E. Anders, ChemBioChem 8 (2007) 530.
[5] M. Ruf, H. Vahrenkamp, Inorg. Chem. 35 (1996) 6571.
[6] (a) K.A. Brown, J.N.B. Bell, Atmos. Environ. 2 (1986) 537;
(b) M. Chin, D.D. Davis, J. Biogeochem. Cycles 7 (1993) 321;
(c) U. Kuhn, A. Wolf, C. Gries, T.H. Nash III, J. Kesselmeier, Atmos. Environ. 34 (2000) 4867.
[7] M.J. Smeulders, T.R.M. Barends, A. Pol, A. Scherer, M.H. Zandvoort, A. Udvarhelyi, A.F. Khadem, A. Menzel, J. Hermans, R.L. Shoeman, H.J.C.T. Wessels, L.P. van den Heuvel, L. Russ, I. Schlichting, M.S.M. Jetten, H.J.M. Op den Camp, Nature 478 (2011) 412.
[8] For CO_2 insertion reactions into cadmium hydroxide complexes, see: (a) R.A. Allred, L.H. McAlexander, A.M. Arif, L.M. Berreau, Inorg. Chem. 41 (2002) 6790;
(b) T. Marino, N. Russo, M. Toscano, J. Am. Chem. Soc. 127 (2005) 4242;
(c) L.-Y. Kong, H.-F. Zhu, Y.-Q. Huang, T. Okamura, X-H. Lu, Y. Song, G.-X. Liu, W.-Y. Sun, N. Ueyama, Inorg. Chem. 45 (2006) 8098;
(d) D.E. Janzen, M.E. Botros, D.G. VanDerveer, G.J. Grant, Dalton Trans. (2007) 5316;
(e) R.A. Allred, S.A. Huefner, K. Rudzka, A.M. Arif, L.M. Berreau, Dalton Trans. (2007) 351.
[9] Y. Xu, L. Feng, P.D. Jeffrey, Y. Shi, F.M. Morel, Nature 452 (2008) 56.
[10] A.E. Eriksson, T.A. Jones, A. Liljas, Proteins Struc. Funct. Genet. 4 (1988) 274.
[11] A. Looney, R. Han, I.B. Gorrell, M. Cornebise, K. Yoon, G. Parkin, A.L. Rheingold, Organometallics 14 (1995) 274.
[12] M. Rombach, H. Vahrenkamp, Inorg. Chem. 40 (2001) 6144.
[13] J. Notni, H. Görls, E. Anders, Eur. J. Inorg. Chem. (2006) 1444.
[14] Just prior to submission of this manuscript, an article (E. Galardon, A. Tomas, P. Roussel, I. Artaud, Eur. J. Inorg. Chem. (2010) 3797–3801) was published online (on 8/1/2011) that described the preparation and characterization of [(TPA)Zn-SH]X (X = ClO_4^- or BPh_4^-). The authors prepared [(TPA)Zn-SH]X (X = ClO_4^- or BPh_4^-) complexes by reacting $[(TPA)ZnOH_2]X_2$ with KSH in methanol.
[15] N.N. Murthy, K.D. Karlin, J. Chem. Soc., Chem. Commun. (1993) 1236.
[16] (a) G. Anderegg, E. Hubmann, N.G. Podder, F. Wenk, Helv. Chim. Acta 60 (1977) 123;
(b) C. Chuang, K. Lim, Q. Chen, J. Zubieta, J.W. Canary, Inorg. Chem. 34 (1995) 2562.
[17] J.C. Mareque Rivas, S.L. Hinchley, L. Metteau, S. Parsons, Dalton Trans. (2006) 2316.
[18] J.W. Canary, Y. Wang, R. Roy Jr., L. Que Jr., H. Miyake, Inorg. Synth. 32 (1998) 70.
[19] C.S. Allen, C. Chuang, M. Cornebise, J.W. Canary, Inorg. Chim. Acta 239 (1995) 29.
[20] Z. Otwinowski, W. Minor, Methods Enzymol. 276 (1997) 307.
[21] A. Altomare, M.C. Burla, M. Camalli, G.L. Cascarano, C. Giacovazzo, A. Guagliardi, A.G.G. Moliterni, G. Polidori, R. Spagna, J. Appl. Crystallogr. 32 (1999) 115.
[22] G.M. Sheldrick, SHELXL-97: Program for the Refinement of Crystal Structures, University of Göttingen, Germany, 1997.
[23] GAUSSIAN 03, Revision D.01, M.J. Frisch, G.W. Trucks, H.B. Schlegel, G.E. Scuseria, M.A. Robb, J.R. Cheeseman, J.A. Montgomery Jr., T. Vreven, K.N. Kudin, J.C. Burant, J.M. Millam, S.S. Iyengar, J. Tomasi, V. Barone, B. Mennucci, M. Cossi, G. Scalmani, N. Rega, G.A. Petersson, H. Nakatsuji, M. Hada, M. Ehara, K. Toyota, R. Fukuda, J. Hasegawa, M. Ishida, T. Nakajima, Y. Honda, O. Kitao, H. Nakai, M. Klene, X. Li, J.E. Knox, H.P. Hratchian, J.B. Cross, C. Adamo, J. Jaramillo, R. Gomperts, R.E. Stratmann, O. Yazyev, A.J. Austin, R. Cammi, C. Pomelli, J.W. Ochterski, P.Y. Ayala, K. Morokuma, G.A. Voth, P. Salvador, J.J. Dannenberg, V.G. Zakrzewski, S. Dapprich, A.D. Daniels, M.C. Strain, O. Farkas, D.K. Malick, A.D. Rabuck, K. Raghavachari, J.B. Foresman, J.V. Ortiz, Q. Cui, A.G. Baboul, S. Clifford, J. Cioslowski, B.B. Stefanov, G. Liu, A. Liashenko, P. Piskorz, I. Komaromi, R.L. Martin, D.J. Fox, T. Keith, M.A. Al-Laham, C.Y. Peng, A. Nanayakkara, M. Challacombe, P.M.W. Gill, B. Johnson, W. Chen, M.W. Wong, C. Gonzalez, J.A. Pople, Gaussian, Inc., Wallingford, CT, 2004.
[24] M. Dolg, U. Wedig, H. Stoll, H. Preuss, J. Chem. Phys. 86 (1987) 866.
[25] J. Tao, J.P. Perdew, V.N. Staroverov, G.E. Scuseria, Phys. Rev. Lett. 91 (2003) 146401.
[26] GAUSSIAN NBO Version 3.1, E.D. Glendening, J.K. Badenhoop, A.E. Reed, J.E. Carpenter, J.A. Bohmann, C.M. Morales, F. Weinhold, Theoretical Chemistry Institute, University of Wisconsin, Madison, WI, 2001; <http://www.chem.wisc.edu/~nbo5>.
[27] N.W. Aboelella, S.V. Kryatov, B.F. Gherman, W.W. Brennessel, V.G. Young Jr., R. Sarangi, E.V. Rybak-Akimova, K.O. Hodgson, B. Hedman, E.I. Solomon, C.J. Cramer, W.B. Tolman, J. Am. Chem. Soc. 126 (2004) 16896.
[28] M.F. Brown, B.F. Gherman, Theor. Chem. Acc. 128 (2011) 137.
[29] R.G. Parr, W. Yang, Density Functional Theory of Atoms and Molecules, Oxford University Press, New York, 1989.
[30] (a) C. Bergquist, G. Parkin, Inorg. Chem. 38 (1999) 422;
(b) H. Brombacher, H. Vahrenkamp, Inorg. Chem. 43 (2004) 6042.
[31] A.G. Blackman, Eur. J. Inorg. Chem. (2008) 2633.
[32] For example, see: (a) M. El-Khateeb, H. Goerls, W. Weigand, Inorg. Chim. Acta 359 (2006) 3985;
(b) D.J. Darensbourg, W. Lee, A.L. Phelps, E. Guidry, Organometallics 22 (2003) 5585;
(c) M. El-Khateeb, K.J. Asali, A. Lataifeh, Polyhedron 22 (2003) 3105;
(d) J.E. Drake, J. Yang, Canadian J. Chem. 78 (2000) 1214;
(e) J.E. Drake, J. Yang, Canadian J. Chem. 76 (1998) 319;
(f) V.-C. Arunasalam, D.M.P. Mingos, J.C. Plakatouras, I. Baxter, M.B. Hursthouse, K.M.A. Malik, Polyhedron 14 (1995) 1105;
(g) D.J. Darensbourg, B.L. Mueller, C.J. Bischoff, S.S. Chojnacki, J.H. Reibenspies, Inorg. Chem. 30 (1991) 2418;
(h) R.J. Magee, M.J. O'Connor, Inorg. Chim. Acta 5 (1971) 554.
[33] (a) R. Baggio, A. Frigerio, E.B. Halac, D. Vega, M. Perec, J. Chem. Soc., Dalton Trans. (1992) 1887;
(b) U. Brand, H. Vahrenkamp, Inorg. Chem. 34 (1995) 3285;
(c) B.S. Chohan, S.C. Shoner, J.A. Kovacs, M.J. Maroney, Inorg. Chem. 43 (2004) 7726.
[34] M. Rombach, H. Brombacher, H. Vahrenkamp, Eur. J. Inorg. Chem. (2002) 153.
[35] (a) M. Mikuriya, X. Jian, S. Ikemi, T. Kawahashi, H. Tsutsumi, A. Nakasone, J. Lim, Inorg. Chim. Acta 312 (2001) 183;
(b) T. Vossmeyer, G. Reek, B. Schulz, L. Katsikas, H. Weller, J. Am. Chem. Soc. 117 (1995) 12881;
(c) R.A. Santos, E.S. Gruff, S.A. Koch, G.S. Harbison, J. Am. Chem. Soc. 112 (1990) 9257;
(d) A.D. Watson, C. Pulla Rao, J.R. Dorfman, R.H. Holm, Inorg. Chem. 24 (1985) 2820.
[36] R. Alsfasser, M. Ruf, S. Trofimenko, H. Vahrenkamp, Chem. Ber. 126 (1993) 703.
[37] D.C. Bebout, S.W. Stokes, Inorg. Chem. 38 (1999) 1126.
[38] S. Mangani, K. Håkansson, Eur. J. Biochem. 210 (1992) 867.